EARTHQUAKE ENGINEERING AND STRUCTURAL DYNAMICS, VOL. 27, 29–47 (1998)

EVALUATION OF THE PERFORMANCE OF A SUSPENSION ISOLATION SYSTEM SUBJECTED TO STRONG GROUND MOTION

A. BAKHSHI*, H. ARAKI AND T. SHIMAZU

Shimazu Laboratory, Department of Structural Engineering, Hiroshima University, Higashi-Hiroshima 739, Japan

SUMMARY

This study is concerned with a new isolation device called a Suspended Pendulum Isolation (SPI) system here. Particular attention is given to evaluate the dynamic behaviour of the system under substantial ground motions including the El Centro 1940, Hachinohe 1968 and Kobe 1995 earthquakes. Shaking-table tests have been carried out for a $\frac{4}{25}$-scaled model comprising a test structure supported on the SPI system with lead damper. Several yield strengths for the lead damper are examined to investigate its properly designed dimensions. Experimental results show that the SPI system with lead damper has a substantial capability to decrease either peak acceleration or peak base (bearing) displacement responses for broad-band frequency excitations. It also confirms that maximum-storey drift index of isolated structure has been dropped to about one-sixth of its corresponding value at fixed-base condition under strong level of predominant excitation along with considerable decrease of peak acceleration. A non-linear analytical model for an MDOF shear building has been also developed by utilizing the fourth-order Runge–Kutta algorithm. Comparison of analytical and experimental time-history responses for all of the excitations indicates that there is a good agreement in both peak values and shape pattern of the results. Moreover, SPI with an appropriate yield strength of lead damper creates only a very small permanent displacement after strong excitation. © 1998 John Wiley & Sons, Ltd.

Earthquake Engng. Struct. Dyn., **27**, 29–47 (1998)

KEY WORDS: seismic isolation; suspended pendulum system; energy dissipator; lead damper; shaking-table experiment; non-linear analysis

INTRODUCTION

Classification of the earthquake-proof structures into two main categories; high-resistant structures and vibration-controlled structures, and the latter to two sub-groups—active and passive control including base-isolation technique, can manifest the basis of two global statements. It is well known that the strengthening strategy inevitably leads to larger masses and, hence, higher seismic forces for the highly seismic risk regions. Also, strong earthquakes may bring remarkable damage on even very stiff structures along with its sensitive internal equipment, in which peak structural acceleration at upper floors usually becomes several times larger than peak ground acceleration. Moreover, the economical consideration does not allow to construct a completely safe structure within the bounds of traditional design method.[1–3]

* Correspondence to: Ali Bakhshi, Shimazu Laboratory, Department of Structural Engineering, Hiroshima University, 1-4-1 Kagamiyama, Higashi-Hiroshima 739, Japan.

Contract grant sponsor: Dainihondoboku Co.
Contract grant sponsor: Japan Ministry of Education; Contract grant number: G08044152

CCC 0098–8847/98/010029–19$17·50

Received 2 April 1997
Revised 20 August 1997

On the other hand, there are some vital structures such as hospitals, fire and relief stations, high-way bridges, and so on, that should be on-service just after any natural disaster, including strong earthquakes. Besides, failure of nuclear-related structures may originate a catastrophe to human race. As a consequence, control systems, in general, and seismic isolation category, in particular, have acquired significant attention in recent years.

A world-wide review on historical development and interpretation of dynamic responses for the various types of isolation systems are provided by Kelly,[1,4,5] Buckle,[6] Skinner,[7] Ahmadi,[3,8] Zayas,[9,10] and their co-workers. Accordingly, lead rubber bearing (LRB) and friction-pendulum system (FPS) are among the top leading techniques of the so-called base-isolation methodology. Although LRB and FPS systems enjoy a variety of advantages, two major disadvantages remain to be solved, i.e. permanent displacement after strong shaking, in addition to high cost because of manufacture and maintenance operations.

A new isolation technique, SPI system, has been innovated by Konishi and Shimazu very recently.[11] In this system, the isolation aim can be achieved by mounting the superstructure on suspending pendulum bearing as a means of decoupling from ground. It provides a horizontally flexible interface between the building and ground at the foundation level, so that the whole system primarily moves as almost a rigid-body motion by a predetermined fundamental period based on the simple principle of a pendulum.[12] The SPI system takes advantage of stability under vertical loads regardless of the amplitude of displacement, besides its simplicity in design, manufacture and installation procedures.

Like other isolation systems, an energy absorber is necessary to prevent the SPI system from large displacement at bearing, in addition to attenuating the transmission of acceleration to the structure. For this purpose, several damping materials including lead, silicone and sponge are examined.[13–15] Herein, results of U-shape-designed lead damper considered as a practical method are presented. Its optimum yield strength which is a key parameter in design has been also investigated. To evaluate the force–displacement characteristics of the SPI system with various yield levels of lead damper, corresponding hysteresis loops of the system under sinusoidal wave are studied.

In the experimental test series, a $\frac{4}{25}$-scale model consisting of a generalized test structure supported on a SPI system accompanied by a lead damper is used. To provide a basis for the comparison of its efficiency, two conditions of SPI without damper and fixed-base bearings have also been tested. Most of the discussions are made for acceleration transmitted to the isolated structure and bearing displacement responses under strong level (50 kine) of excitations. A non-linear program based on the Runge–Kutta algorithm has been developed for a multi-degree-of-freedom system. Results of the experiment and analysis are compared and discussed for some important cases.

GOVERNING EQUATION OF MOTION AND MODELING

The SPI isolation system comprises a base-plate hung from circularly arranged bolts over a precast box so that the whole suspending system oscillates as a simple pendulum, as shown in Figure 1. Its natural period of vibration is controlled only by the selection of suspending length, l, and is independent of weight. Gravity load makes it respond as a conservative system that any change caused by external forces is self-returnable to the preexcited position. The equation governing the motion of SPI system in Figure 1 can be given as

$$m_b\ddot{x}_b + C_o\dot{x}_b + K_b x_b = -m_b\ddot{x}_g \tag{1}$$

where m_b is the lumped mass of the pendulum, C_o the inherent damping coefficient, K_b the restoring stiffness, x_b the relative displacement of pendulum base to the ground and $\ddot{x}_g$ is the base ground acceleration. The term $K_b x_b$ is a horizontal force that produces the displacement x_b, and may be given by summation of moment over point O in Figure 1(b) or $\sum M_o = 0$.

$$K_b x_b = m_b g \tan\theta \tag{2}$$

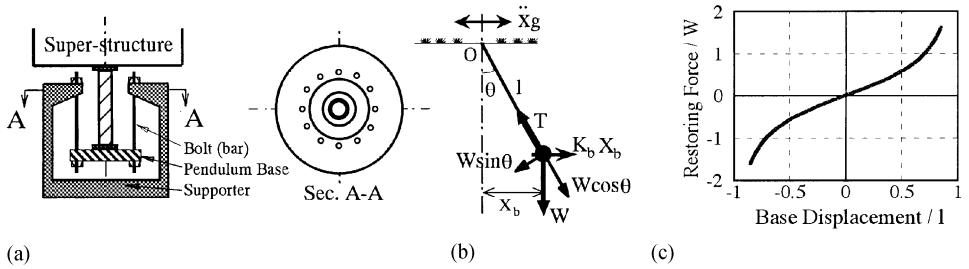

Figure 1. Model of the suspended pendulum isolation (SPI) system: (a) developed SPI device; (b) force diagram; and (c) force–displacement relationship

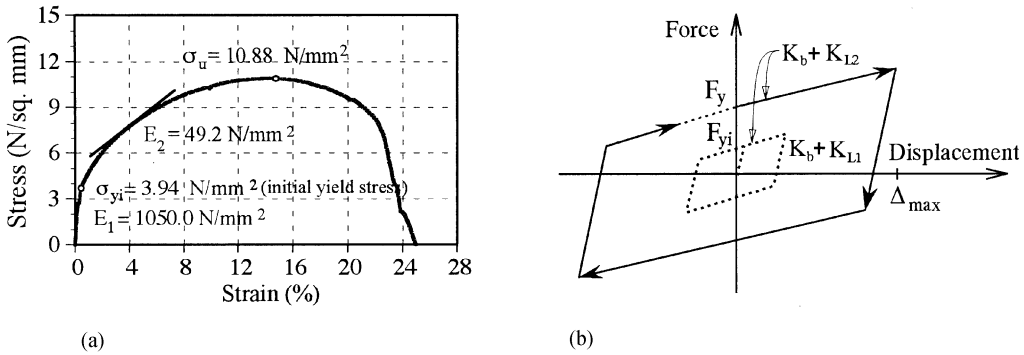

Figure 2. Stress–strain relationship of lead and its corresponding analytical model: (a) Experimental result of σ-ε; and (b) proposed hysteresis loops in analysis

where g is gravity acceleration and θ the angle of rotation, as $\theta = \arcsin(x_b/l)$ in which l is the suspending length of pendulum. It is important to note that in this study, very slender bars (wire) are assumed to be used.

Hence, the circular frequency of the system, ω, which may be basically defined as the square root of stiffness over mass, results in the following approximation:

$$\omega \cong \omega_o[1 + 0{\cdot}75(x_b/l)^2 + \cdots] \tag{3}$$

where ω_o is the linear approach of frequency equal to $\sqrt{g/l}$ that accounts for small values of angle θ.

Equation (3) indicates that the frequency of the system is dependent on the amplitude of oscillation and is larger than the linear one for non-zero values of x_b. However, the displacement capacity of bearings by introducing energy dissipator are primarily designed to be $x_b < 0{\cdot}2l$, thus the resulting error in the linearized model may be less than 5 per cent.

To control bearing displacement, several dampers such as silicone, sponge and lead materials were investigated in previous studies.[11–15] Among them the lead damper is found to be the best alternative from both practical and economical viewpoints. Figure 2(a) shows the experimental stress–strain curve of unitension test for lead specimens. As indicated in this figure, lead metal has an almost elastoplastic behaviour with a significantly large range of strain, which provides an effective hysteretic damping for the system. However, increasing stress level after initial yield should not be omitted.

Figure 2(b) displays the force–displacement relationship considered in the analysis for SPI accompanied with a lead damper, based on combination of Figures 1(c) and 2(a). It shows that yield force is varied from an initial yield level (dash-line loop) depending on the stress level of the lead damper corresponding to the maximum cyclic displacement.

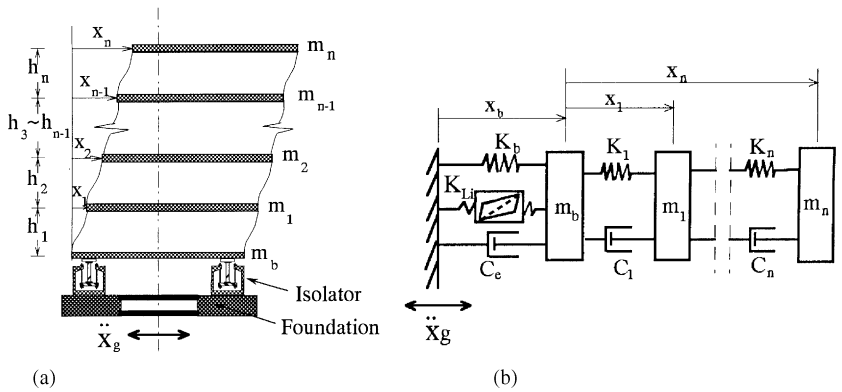

Figure 3. Multi-storey frame structure mounted on SPI system including the lead damper: (a) structural model supported on SPI; and (b) Schematic view of model

Based on Figure 3, the coupled equations of motion for a multi-storey shear frame supported on the SPI system can be derived as

$$M\ddot{x}_b + C_o\dot{x}_b + (Mg\tan\theta + K_{Li}x_b) + \sum_{i=1}^{n} m_i\ddot{x}_i = -M\ddot{x}_g \tag{4}$$

$$[m]\{\ddot{x}\} + [c]\{\dot{x}\} + [k]\{x\} = -[m]\{I\}(\ddot{x}_g + \ddot{x}_b) \tag{5}$$

where M is the total mass of the entire oscillating system, x_i the displacement of the ith floor of the structure relative to the base that represents the component of vector $\{x\}$, and K_{Li} is additional stiffness arising from damping system, e.g. K_{L1} and K_{L2} as pre- and post-yield stiffness for lead metal, respectively. Matrices $[m]$, $[c]$ and $[k]$ symbolize structural mass, damping, and stiffness, respectively. Here, a dot on top of the letters denotes a time derivation and $\{I\}$ is a unity column vector.

As a reference, it is important to estimate the equivalent viscous damping of a hysteretic system and its effective period. For this purpose, equation (4) can be rewritten as follows:

$$M\ddot{x}_b + C_e\dot{x}_b + K_e x_b + \sum_{i=1}^{n} m_i\ddot{x}_i = -M\ddot{x}_g \tag{6}$$

where $C_e = C_L + C_o$ is the effective viscous damping coefficient of an equivalent linear system and K_e is the secant modulus from extreme negative-to-positive base displacement of each cycle. To calculate the equivalent viscous damping C_L the following formula can be used:

$$C_L = W_d/\pi\omega_e\Delta_{max}^2 \tag{7}$$

in which W_d is the energy dissipated in a hysteresis loop with maximum displacement of Δ_{max}, and ω_e^2 is ratio of K_e to total mass M. It is obvious that the addition of hysteretic damping strengthens the stiffness of the system, and thus shortens its effective period ($T_e = 2\pi/\omega_e$) compared to that without the damper. As a consequence, yield strength of the lead damper is a key parameter in design which influences both T_e and Δ_{max}.

Equations (4) and (5) discussed before are general to model the shear building for developing a computer program. In order to provide an appropriate accuracy for the mentioned non-linear problem, the Runge–Kutta scheme, which is one of the efficient and stable methods,[16] has been utilized in the numerical procedure and then verified by shaking-table results.

TESTING METHOD AND ITS VERIFICATION

A natural period of 2 s or larger has been gained in most of the other types of base isolators such as lead rubber bearing (LRB), resilient-friction (R-FBI), friction-pendulum system (FPS), etc.[7,9] In this new isolation system also the trade-off between reducing acceleration and, as a result, increasing base displacement when fundamental period increases, leads to a predominant period of 2 s and hence to a pendulum length of 1·0 m.[11,12] The pendulum length of 16 cm in the model compared to 100 cm in the prototype, resulting in a $\frac{4}{25}$ length scale model, has been considered in this experimental research. It should be noted that input earthquakes needed to be compressed by a time-scale factor of $\frac{2}{5}$ according to the simulation law.

A generalized one-storey test structure with a fundamental period of 0·162 s (0·405 s in prototype size) has been selected as a representative of low-rise building without bringing into consideration its higher mode effects. To evaluate the effectiveness of the new SPI system, the result of fixed-base (conventional) structure has been also examined. It is necessary to mention that since the simulation law for the test structure as a shear building is satisfied by considering its fundamental period, results of the structure itself, i.e. drift index, should be interpreted carefully when extrapolating such results to prototype structures.

The NS component of El Centro 1940, Hachinohe 1968, and Hyogoken–Nanbu (Kobe) 1995 ground motions are used. All the input accelerograms are adjusted to have a maximum velocity of 25 and 50 cm/s according to Japanese design criteria for weak and strong levels of an earthquake.[4,17,18] However, most of the discussions are made about strong level in order to emphasize the effectiveness of the new device. Table I shows input peaks of three earthquakes scaled for 50 kine. It is obvious that a factor of time scale equal to f_{ts} modifies the input velocities by f_{ts} and the input displacements by f_{ts}^2 factors when the acceleration level of the scaled model are identical to the prototype size. Note that the values shown in parentheses denote those amounts corresponding to the time scaling of $\frac{2}{5}$ considered in present study.

Figure 4 illustrates the photograph of the testing model consisting of a generalized test structure supported on the SPI system. It shows an isolated structure mounted on a pendulum bearing which is supported at its four corners. Figure 1(b) shows a close-up view of its lead damper. As displayed in this figure, lead elements (rectangular section) are fixed at the end against rotation which produces a uniform shear force along its height. This U-shaped damper provides the advantage of permitting vertical movement which is necessary for pendulum oscillation.

Figure 5 describes the procedure of experimental tests schematically. As shown in this figure, acceleration and displacement output at top of the test structure, base of the pendulum (bearing), and top platform of the shaking table in a horizontal direction have been recorded. Detail A-1 in Figure 5 displays a sample of lead damper being used in the experiment which is basically designed for unidirectional operation. However, for full-scale structures in which the damper should be conforming with the isolation system operating in all directions, it is feasible to design dampers of a circular section. It is also possible to utilize multi-layer damper (presented here) with proper end supports activating only in one of the principal axes of building. In the latter case, two perpendicular components can provide appropriate damping forces for the multi-directional movement.

Sizes and dimensions of lead segments were designed to have four levels of yield strength, i.e. from 2·5 to 10·0 per cent, compared to the total weight (W) of the superstructure including the pendulum base. Figure 6

Table I. Peak values of input earthquakes adjusted to 50 kine

Input Earthquakes	Acceleration (cm/s^2 or gal)	Velocity (cm/s or kine)	Displacement (cm)
El Centro	504·861	50·0 (20·0)	− 16·332 (− 2·613)
Hachinohe	342·940	− 50·0 (− 20·0)	14·158 (2·265)
Kobe	− 451·397	50·0 (20·0)	11·155 (1·785)

may simply point out the assessment for a single part of the lead damper under a force F acted by the base of the SPI bearing. Yield force has been considered as the force that produces stress of $\sigma = \sigma_y$ at points A and C, as shown in Figure 6(c). Condition of $\sigma = \sigma_u$ is judged for the ultimate capacity of the system which makes the upper limit for x_b based on the ductility factor. An explicit analysis involving geometric and material non-linearity verified that x_b, peak base displacement corresponding to even yield strength of 2·5 per cent W under strong level of excitations, remains below the stated limitation.

To determine the optimum yield strength for the lead damper, minimal of peak base shear coefficient of the isolated structure along with the peak-bearing displacement ratio (max of x_b/l) under strong level (50 kine) of excitations are recognized as the main target. Figure 7 illustrates the results of the experiment for the mentioned yield ranges. Result of each yield strength shown in this figure corresponds to the average value resulting from several tests for every excitation. It is perhaps interesting to note that nearly similar results to Kobe's curves were acheived under sine wave at the resonant period.

It shows that increasing yield strength decreases both peak base shear coefficients and bearing displacement ratios up to about 7·5 per cent W. For further increase, however, peak base shear trends to be raised notably because of the increase in peak acceleration at the top of the structure, while its advantage of displacement reduction is insignificant. This is in agreement with the fact that increase of yield strength increases the effective damping ratio (see Table II) but decreases the effective period of the system due to the additional rigidity of the lead damper. As a result, it leads to a conclusion that yield strength of 7·5 per cent W is the most appropriate value for this survey, so that discussion in the next sections are specially about this value.

Bandwidth (half-power) and free-vibration methods have been carried out to identify the dynamic characteristics of the SPI system with the lead damper for each yield strength with a variety of amplitudes. It confirmed that the effective damping ratio of the lead damper and effective period of the system would be dependent on amplitude of oscillation. Table II gives a brief abstract on the results of four successive levels,

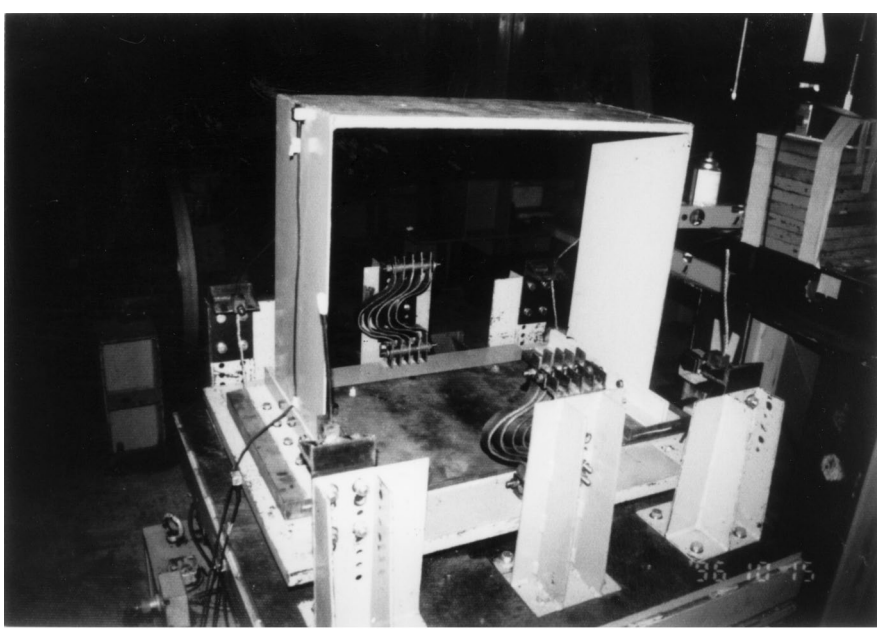

(a)

Figure 4. Testing model of SPI installed on a shaking table: (a) photograph of test structure supported by SPI

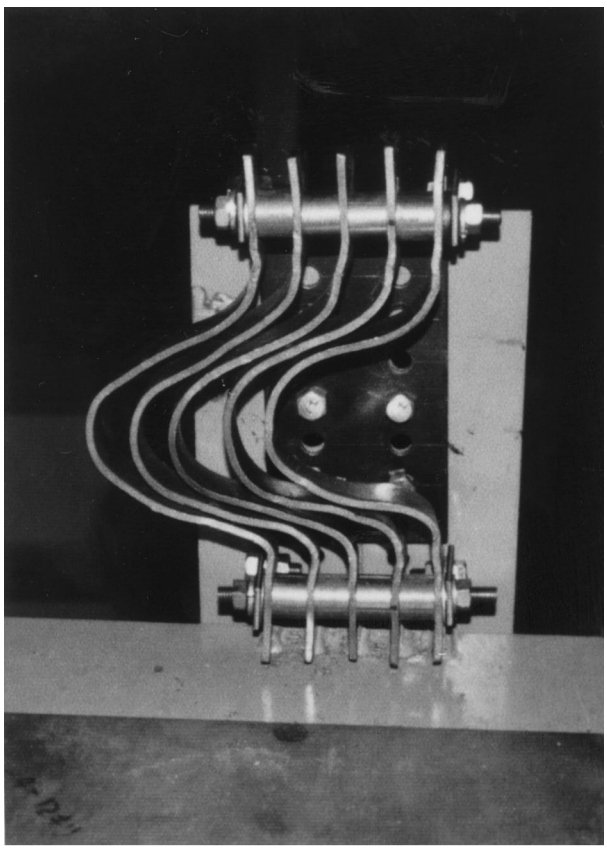

(b)

Figure 4(b). Photograph of lead damper

e.g. portion of 2·5 per cent W. Accordingly, the damping ratios and natural periods concluded in Table II are average values of a series of experiment for such peak amplitudes as strong level of earthquakes, 50 cm/s.

Figure 8, as a sample, shows results of the SPI system with lead-1 and lead-3 dampers for relatively large amplitudes. Figure 8(a) illustrates amplitude of the SPI bearing displacement responses exciting under sinusoidal input wave for two yield ratios of 2·5 per cent W and 7·5 per cent W. It indicates that the resulting curve of the SPI with lead-3 damper has a broader bandwidth (higher damping) and its resonant period is being shifted to the left which implies larger rigidity for the system, compared to the results of SPI with lead-1 damper. From Figure 8(b), one may easily reach a conclusion that the effective viscous damping ratio of lead-3 ranges from 25·6 to 17·1 per cent of critical damping when the amplitude degrades from 50 to 5 mm (or 31·25 to 3·12 cm in prototype size).

To acquire the precise force–displacement characteristic of the SPI system mobilized with various yield levels of lead damper, the experiment is extended to investigate hysteresis loops of the system for sine wave excitation under resonance frequency. Results of the SPI with lead-1–lead-3 and also without damper are shown in Figure 9. It is important to note that this is the result of the last tests, after carrying out a variety of experiments, which was similar to pretest ones. This can be considered as a beneficial property in practice which may offer long durability and thus less cost of upkeep.

Figure 9(a) shows that the relationship between lateral force and displacement is almost linear when the system oscillates without the enhanced damper. As shown in Figures 9(b)–(d), the system responds as a nearly

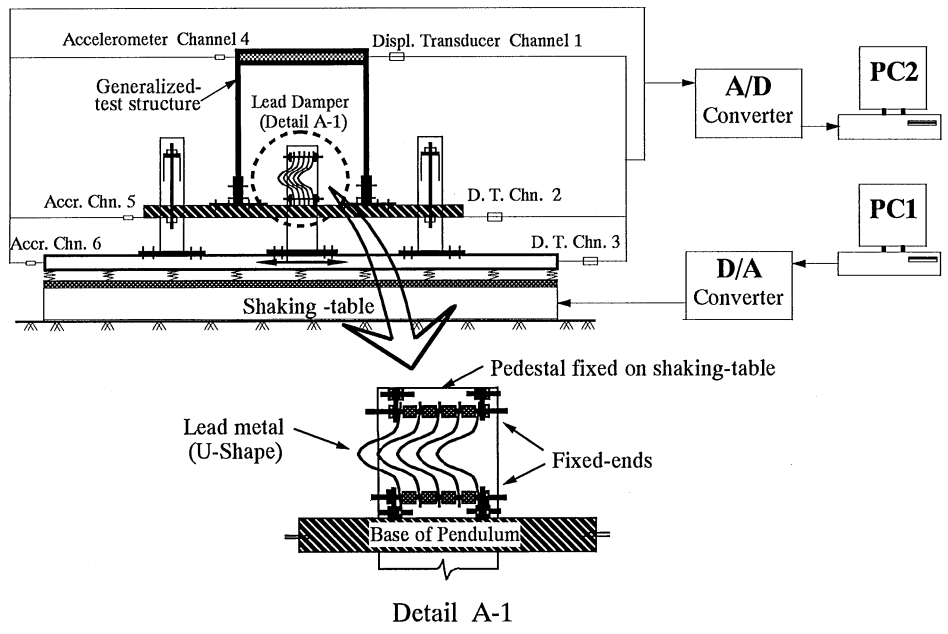

Figure 5. Representative of shaking-table test

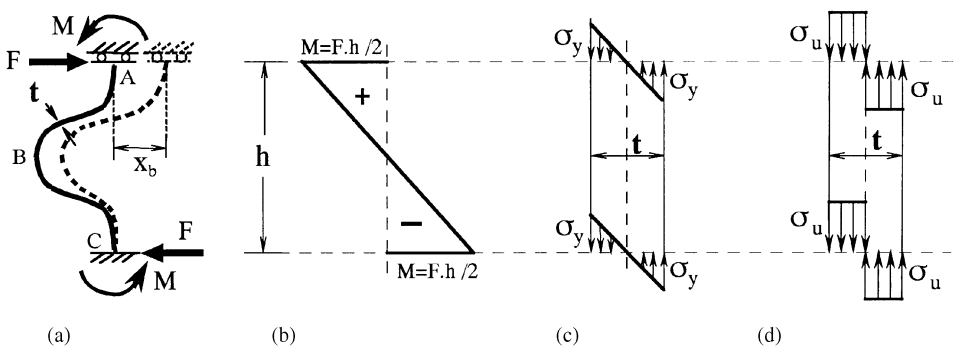

Figure 6. Determination of yield strength for the lead damper: (a) lead element; (b) moment diagram; (c) yield condition; and (d) ultimate condition

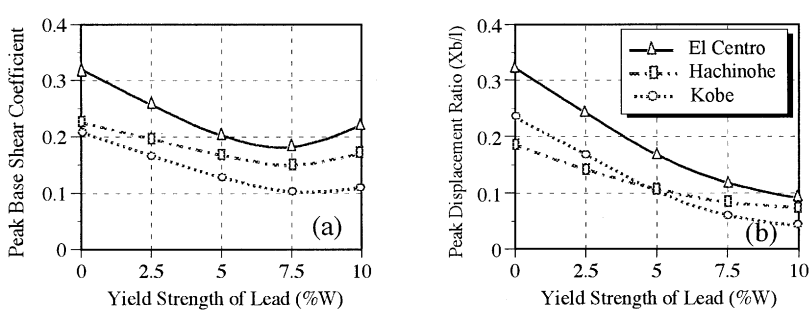

Figure 7. Peak base shear of isolated structure and bearing displacement of SPI system subjected to strong level (50 kine) of excitations versus yield strength of lead damper

Table II. Dynamic characteristics of the SPI system with various yield strength of lead damper

Damping material	None	Lead-1 (2·5 per cent W)	Lead-2 (5·0 per cent W)	Lead-3 (7·5 per cent W)	Lead-4 (10·0 per cent W)
Damped-natural Period (s)	0·785	0·714	0·657	0·573	0·452
Effective damping ratio (per cent)	2·02	7·65	13·94	19·25	23·40

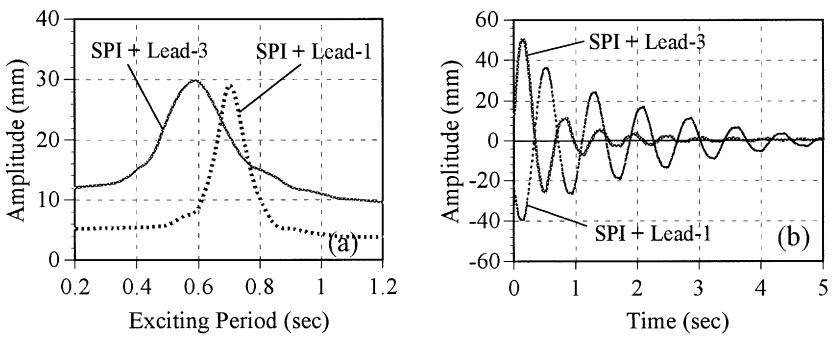

Figure 8. Sample result of identification tests; (a) bandwidth method; and (b) free vibration

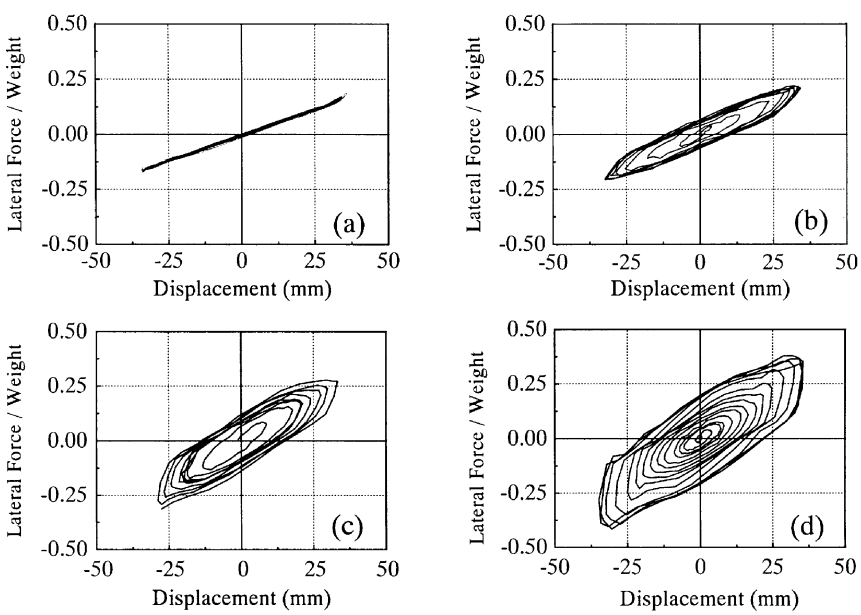

Figure 9. Hysteresis loops of the SPI system under sinusoidal wave excitation, enhanced with: (a) none (b) lead-1 (2·5 per cent W) (c) lead-2 (5·0 per cent W) and (d) lead-3 (7·5 per cent W) dampers

bilinear stiffness property which is consistent with the proposed model in the analysis. From these figures it is observed that increasing the yield strength of the lead damper expands the hysteresis loops increasingly along the vertical direction which provides more hysteretic damping for the system. It is also observed that typical stiffness of the system increases gradually from Figure 9(a) to Figure 9(d).

EXPERIMENTAL RESULTS

The main purpose of this section is to evaluate the behaviour of the isolated-structure supported on SPI system under major earthquakes that contain specific characteristics. It is well known that peak ground motion, duration of strong shaking, and frequency content are the most important characteristics of an earthquake motion in engineering applications. In this study, fast Fourier transform routine is used to characterize the frequency content of accelerograms.

Figure 10 shows the acceleration time histories and Fourier amplitude spectra for original NS components of El Centro 1940, Hachinohe 1968, and Hyogoken-Nanbu (Kobe) 1995 ground motions. This figure indicates that the strongest energy in El Centro motion is in the period range of 0·5–1 s, while such long periods as 2–3 s in the Hachinohe accelerogram also contain considerable energy of excitation. On the contrary, Kobe ground motion has a particular characteristic of firm media recording that short period of waves between 0·2 and 0·5 s have abundant energy.

A specific observation which can be made from this figure is that the peak Fourier amplitudes are almost the same in spite of their different peak ground acceleration values, in particular the Kobe record whose peak acceleration is nearly three times as large as Hachinohe's. This can be explained by the fact that duration of strong shaking also is a crucial parameter in Fourier analysis.

In the following section, particular attention is given to examine the effectiveness of the SPI system with lead-3 (7·5 per cent W) damper under strong level (50 kine) of three earthquakes.

El Centro responses

Figure 11 compares time histories of the absolute acceleration response ($\ddot{x}_g + \ddot{x}_b + \ddot{x}_1$) at the top of isolated test-structure and relative base displacement of bearing(x_b) on the SPI system with and without

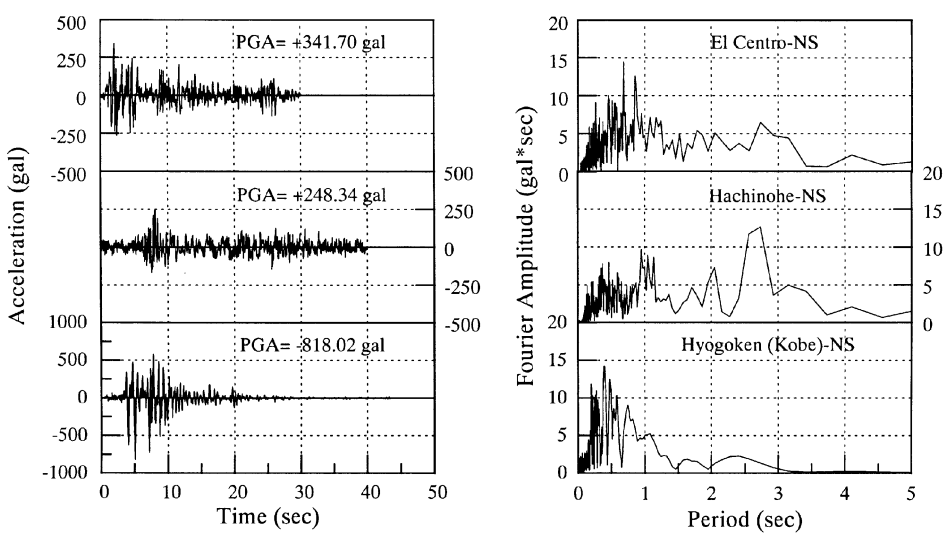

Figure 10. Acceleration time histories of El Centro, Hachinohe and Kobe earthquakes along with their Fourier spectra plotted as a function of period

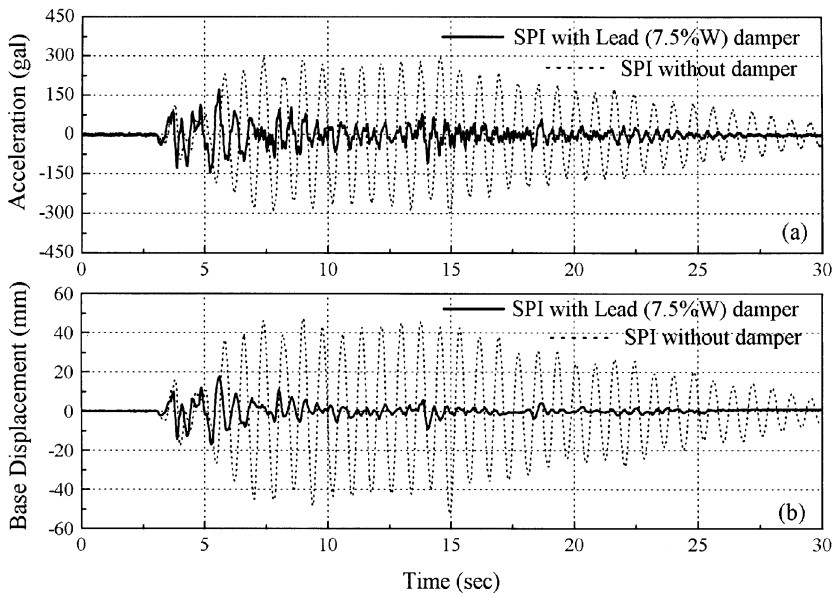

Figure 11. Experimental responses at the top of the isolated structure on the SPI system and its bearing supporter subjected to scaled El Centro (50 kine) excitation

lead-3 (7·5 per cent W) damper under El Centro-NS excitation. This figure shows that peak acceleration response corresponding to the condition of without damper (dash line in Figure 11(a)) has been decreased by about 40 per cent due to period shifting while the peak relative base displacement is increased by nearly 100 per cent, compared to peak input acceleration and displacement, respectively.

The general feature of these responses indicates that usage of lead damper reduces either acceleration or displacement peak values considerably. It also shows that the designed lead damper prevents the system from oscillating as steadily as random sinusoidal amplitudes so that responses have been decreased increasingly after a few sharp peaks at the beginning of strong excitation. These results are due to effect of period shifting by the SPI system in addition to efficient hysteresis damping. As shown in Figure 11(b), by using the lead damper, the maximum relative base displacement has been reduced to 17·7 mm in the model (i.e. 11·1 cm in prototype). It is worth noting here that the latter value is recommended in Japanese design criteria not to exceed 30 cm when LRB has been employed as isolator.[4,17]

It is important to note that the maximum drift index of the isolated structure approached the small value of $\frac{1}{320}$ for the second level of excitation when the SPI had been provided with the lead-3 damper. This conclusion proves that even if the SPI system experiences such El Centro class earthquake; namely peak ground acceleration (PGA) of 0·51g, it can protect the building against considerable damage in which the structure performs in the linear domain of its material properties.

Figure 12 shows the Fourier decomposition of the experimental acceleration responses at the top of isolated structure for various yield strengths of the lead damper and fixed-base condition under El Centro excitation. From Figure 12(a) one may conclude that periods in the range of 0·15–0·25 s contain considerable energy, which is peaked at about 0·162 s corresponding to the fundamental period of the test structure. Comparing this figure with El Centro Fourier spectrum in Figure 10 indicates that fixed-base structure amplifies the peak acceleration response by more than four times the input peak acceleration.

Figure 12(b) shows the Fourier decomposition of the acceleration responses at the top of the isolated structure and its base supporter for the SPI without enhanced damping system. It verifies that the SPI system is filtering out most of frequency contents of input acceleration different from its fundamental period 0·8 s

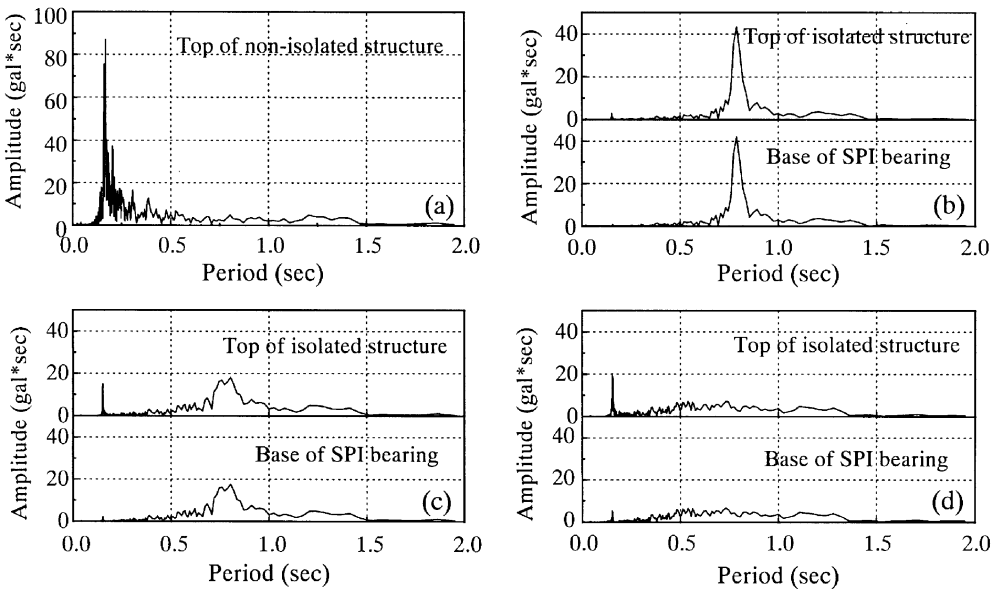

Figure 12. Fourier spectra of acceleration responses examined under El Centro (50 kine) excitation: (a) fixed-base structure, (b) supported by the SPI without damper (c) supported by the SPI with lead-1 (2·5 per cent W) damper and (d) supported by the SPI with lead-3 (7·5 per cent W) damper

(2·0 s in prototype). It verifies that rigid-body motion is valid since Fourier spectra at the top of the isolated structure and its bearing are quite similar.

Figures 12(c) and 12(d) illustrate Fourier spectra of acceleration responses at the top of the isolated structure and its the SPI bearing with lead-1 (2·5 per cent W) and lead-3 (7·5 per cent W) dampers, respectively. It shows that increasing the yield strength of the lead damper develops a sharp peak at a period of 0·162 s which is an influence of structural property to its own response due to additional rigidity by lead. It is also observed that the sharp peak of Figure 12(b) at 0·8 s becomes broader due to damping effect. This characteristic is a desirable property in practice which is believed that it can protect the isolation system from resonating under excitations of long-period contents.

Hachinohe responses

To comprehend the effects of long-period contents of ground excitation on the isolated structure, the accelerogram of the N–S component of Hachinohe 1968 is used. As displayed earlier in Figure 10, the predominant period of Hachinohe accelerogram is ranging from 0·4 to 3·5 s, which comprises the fundamental period of the SPI system too.

Figure 13 shows the absolute acceleration ($\ddot{x}_g + \ddot{x}_b + \ddot{x}_1$) responses at top of the isolated structure on the SPI supporter and its bearing displacement (x_b), subjected to the Hachinohe (50 cm/s) earthquake. From Figure 13(a), it is observed that peak acceleration response at the top of isolated structure for the condition of without damper is reduced by approximately 50 per cent, compared to input peak acceleration, because of only period shifting influence. It also displays that introducing lead damper decreases maximum acceleration responses significantly, regardless of developing a single strong peak at the beginning of strong excitation.

Comparing these results with the corresponding responses of El Centro in Figure 10, clarifies two major differences between them. First, Hachinohe responses of without damper appear as highly random amplitude with sharp peaks, instead of rather smooth sinusoidal responses in El Centro excitation. Secondly, the most

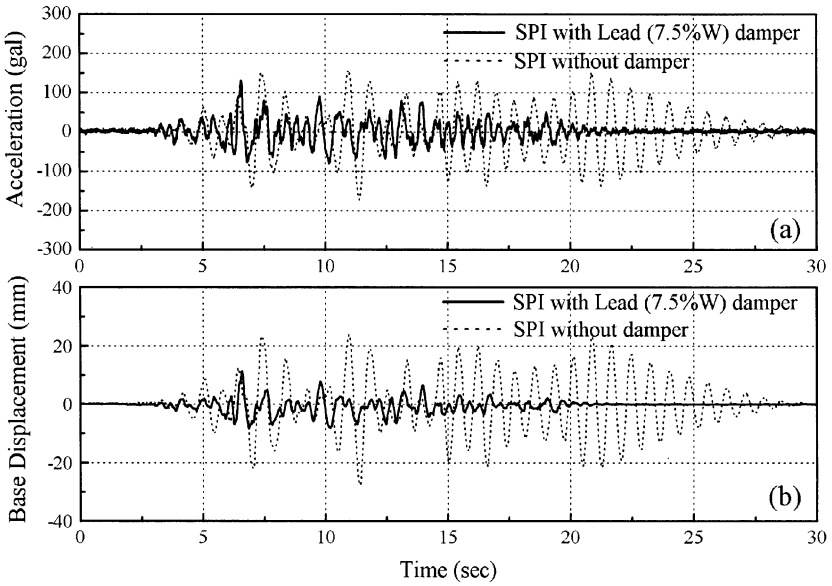

Figure 13. Experimental responses at the top of the isolated structure on the SPI system and its bearing supporter subjected to scaled Hachinohe (50 kine) excitation

energetic part of responses for the SPI without damper under Hachinohe excitation locates at the second half of time histories, i.e. after $t = 15$ s.

Inspite of stated differences, isolation system with lead damper is able to decrease peak base displacement by more than 60 per cent, compared with the corresponding case of without damper. It also proceeds to keep maximum displacement responses in very low level soon after a sharp peak occurring at early stage. Interestingly, SPI system with lead damper eliminates those large responses of SPI without damper at the second half, since its damper has been activated before.

Figure 14 displays the Fourier decomposition of the experimental acceleration responses at the top of the isolated structure under Hachinohe excitation for various yield strength of lead damper and fixed-base condition. Figure 14(a) shows that Fourier spectra of the non-isolated structure peaks at 0·162 s, corresponding to its fundamental period, and its Fourier amplitude peak is larger than that of Figure 12(a). Comparing other results in Figure 14 with Figure 12 indicates that responses resulting from Hachinohe excitation contain broader spectrum which implies more modification for effectiveness of isolation system.

Hyogoken–nanbu (Kobe) responses

Since passive control including base-isolation system was basically innovated to protect low-rise buildings and because predominant period of Kobe earthquake is ranging from 0·2 to 0·5 s, results of the ongoing part can be of notable interest.

Figure 15 illustrates the absolute acceleration responses at the top of isolated structure on the SPI system and relative displacement of bearing for two conditions of with and without lead damper, subjected to Kobe-NS (50 cm/s) accelerogram. It is seen that the SPI system with lead damper dissipates exciting energy very actively which causes about 65 per cent reduction at peak responses in comparison to the case of damper absence.

It is important to note that inter-story drift index of isolated structure approached to $\frac{1}{470}$ which is 13·25 times less than the corresponding value at fixed-base condition, i.e. $\frac{1}{35}$. Therefore, the SPI system performs with more efficiency against Kobe excitation among the discussed three earthquakes.

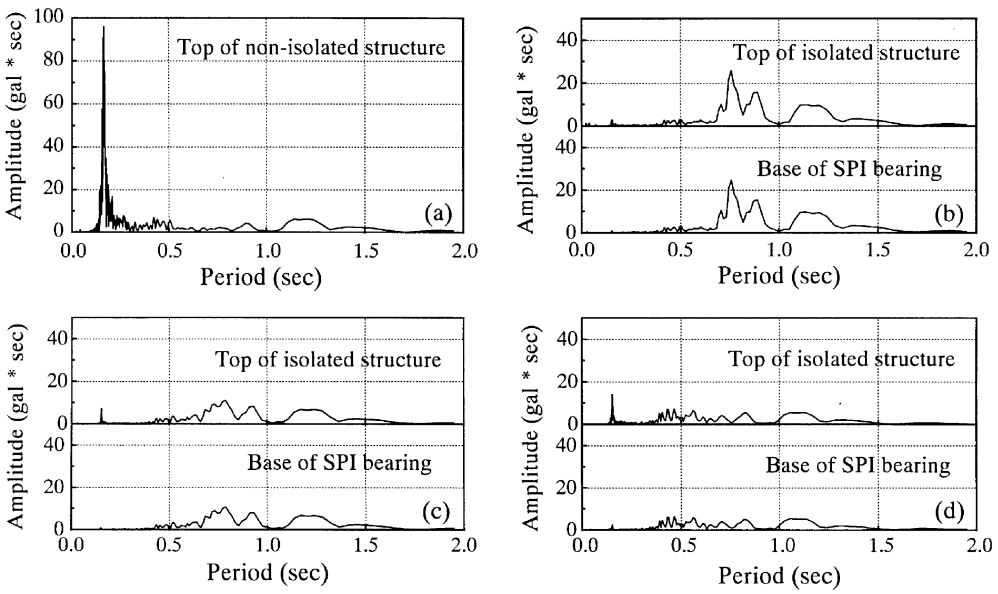

Figure 14. Fourier spectra of acceleration responses examined under Hachinohe (50 kine) excitation: (a) fixed-base structure; (b) supported by SPI without damper; (c) supported by SPI with lead-1 (2·5 per cent W) damper and (d) supported by SPI with lead-3 (7·5 per cent W) damper

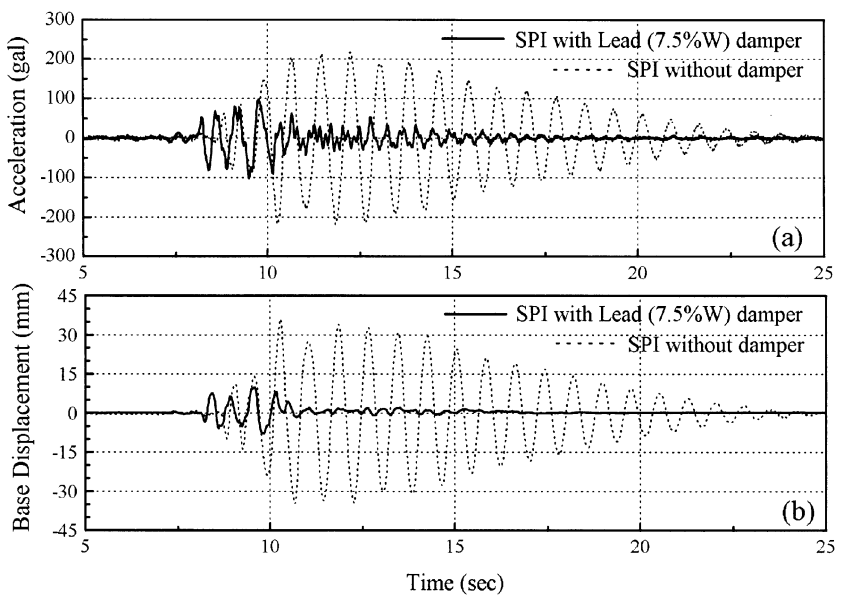

Figure 15. Experimental responses at the top of isolated structure on the SPI system and its bearing supporter subjected to scaled Kobe-NS (50 kine) excitation

CORRELATION BETWEEN ANALYSIS AND EXPERIMENT

In this section, results of the analysis are compared with those of shaking-table experiment. In non-linear procedure, bilinear model for force–displacement relationship of isolation system with lead damper has been considered, as shown in Figure 2(b) and then validated by experiment in Figure 9. Figure 9(d), which is the resulting hysteresis loop for the SPI system accompanying lead-3 (7·5 per cent W) damper under gradual increase of exciting amplitude for sine wave, has provided adequate formulation for establishing relationship between maximum base displacement in each cycle and its corresponding yield level.

Accordingly, yield force F_y is evaluated based on maximum displacement at the beginning (estimation) and end of the cycles (calculation), and then being modified till a proper convergence is acquired. To illustrate accuracy of the proposed analytical model, a few samples are shown and discussed here.

Figures 16 and 17 compare analytical and experimental results of absolute acceleration at the top of the isolated structure on the SPI with lead-3 damper and bearing displacement, subjected to NS components of El Centro and Hachinohe accelerograms, respectively. As shown in these figures, there is a good agreement between analysis and experiment in both peak values and shape pattern. Note that a small variance in starting cycles of vibration regarding analysis exist, specially for El Centro excitation, which is perhaps due to the neglect of round corner effect of the actual hysteresis loops (see Figure 9(d)). Nevertheless, estimation of spectral responses, typically considered as key parameters for design, results in sufficient accuracy.

Figures 18 represents the comparison of analytical and experimental results for lateral force of the SPI system enhanced with lead-3 damper versus its base displacement under El Centro and Hachinohe strong motions (50 kine). This figure again confirms that the proposed model of analysis is able to predict well the experimental responses. Therefore, it is evident that the small variance between analytical and experimental time history responses in Figures 16 and 17 have not lead to remarkable difference in estimation of system characteristic.

Figure 19, collectively, represents experimental and analytical results of spectral responses for using the SPI isolation system with lead-3 damper under increasing input intensities. Figure 19(a) shows the ratio of maximum absolute acceleration responses at the top of the test structure to input peak acceleration

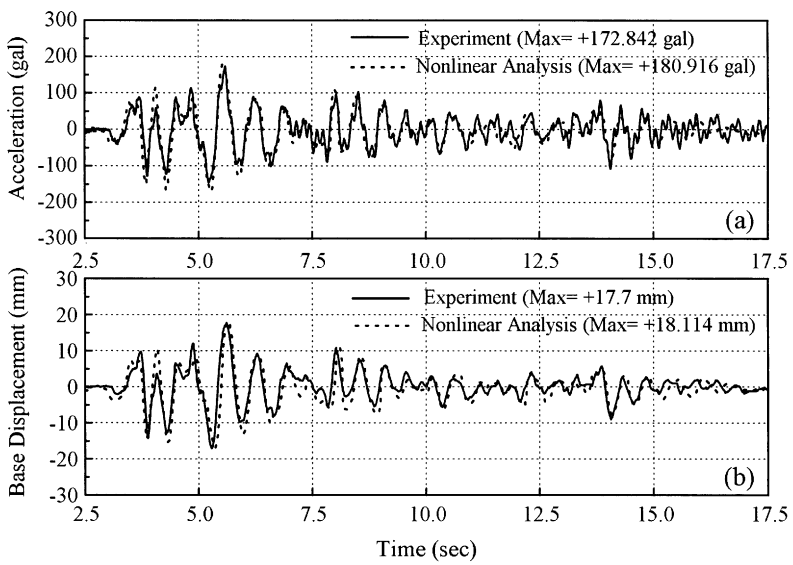

Figure 16. Comparison of analysis with experimental responses at the top of the isolated structure (acceleration) and its the SPI isolator (displacement) under El Centro (50 kine) excitation

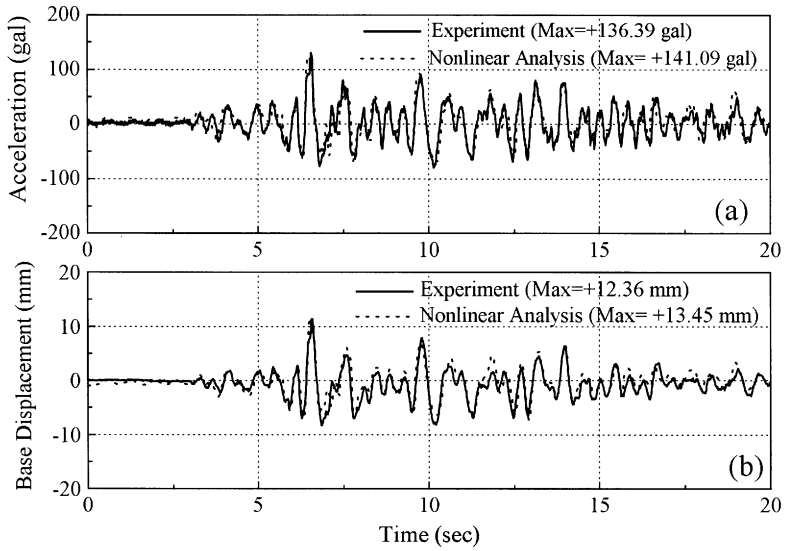

Figure 17. Comparison of analysis with experimental responses at the top of the isolated structure (acceleration) and its the SPI isolator (displacement) under Hachinohe (50 kine) excitation

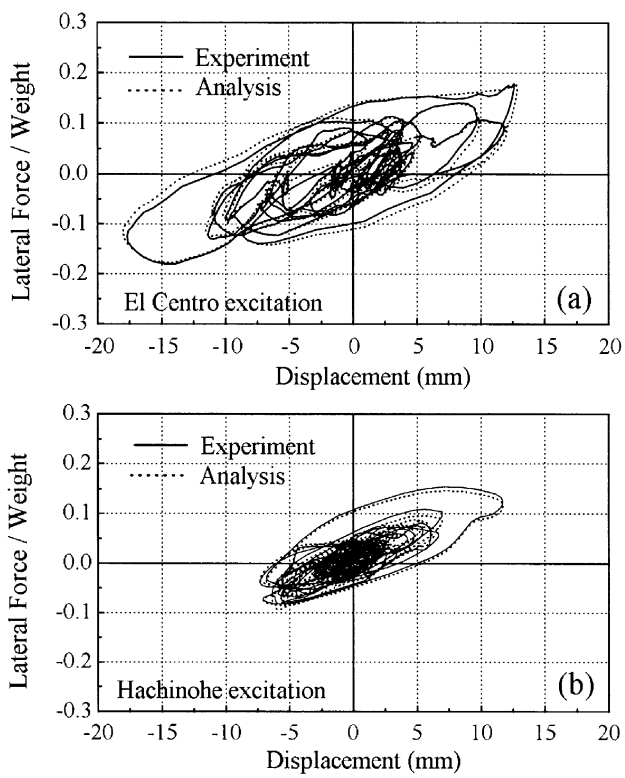

Figure 18. Comparison between hysteresis loops of analytical and experimental responses for the SPI system under (a) El Centro and (b) Hachinohe excitations (50 kine)

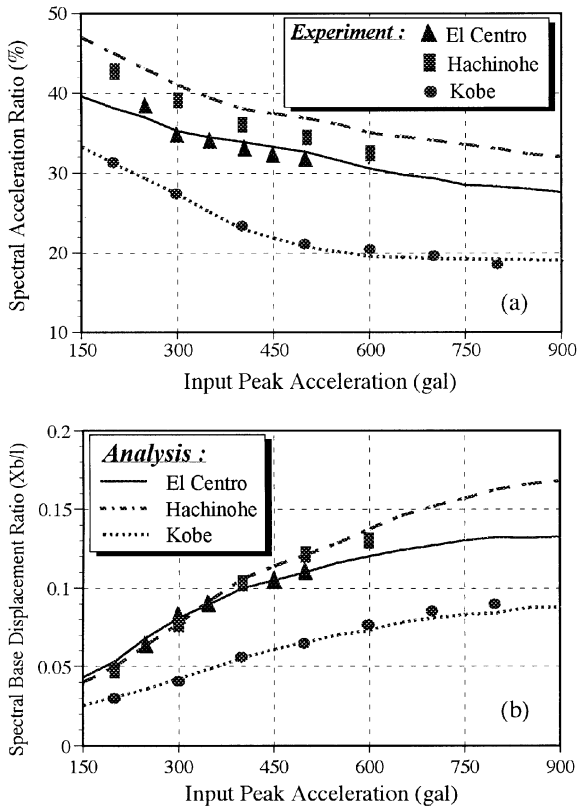

Figure 19. Spectral responses of the SPI system with lead-3 damper subjected to various intensities of El Centro, Hachinohe, and Kobe excitations

$[\max(\ddot{x}_g + \ddot{x}_b + \ddot{x}_1)/\max(\ddot{x}_g)]$ versus input peak acceleration (max of $\ddot{x}_g$) for each of the excitations. Figure 19(b) displays the relationship between the ratio of maximum horizontal bearing displacement to pendulum length (max. of x_b/l) and input peak acceleration.

The first important observation to be made from Figure 19(a) is that the ratio of spectral acceleration responses to input peak acceleration is being decreased while the intensity of input acceleration increases. Also in Figure 19(b), when intensity of input excitations increase the slope of increase on spectral base displacement decreases, specially for stronger level than $0{\cdot}5g$. It means that the effectiveness of the isolation system increases apparently with increasing input intensity. These can be explained by the fact that lead because of its higher hysteresis damping in larger amplitudes provides more reduction in responses under strong levels of excitation.

Another substantial observation to be concluded is that the analytical model predicts adequately the peak experimental responses for all of broad-band excitations. It is perhaps of interest to note that the order of magnitude of error in estimation of maximum responses is less than 5 per cent.

Response spectra

To comprehend the effect of structural natural period on its own responses and isolator, the proposed analytical model including higher mode effect has been considered in this section. The normalized El Centro, Hachinohe, and Kobe accelerograms (1000 gal) are used to evaluate the maximum responses of a structure

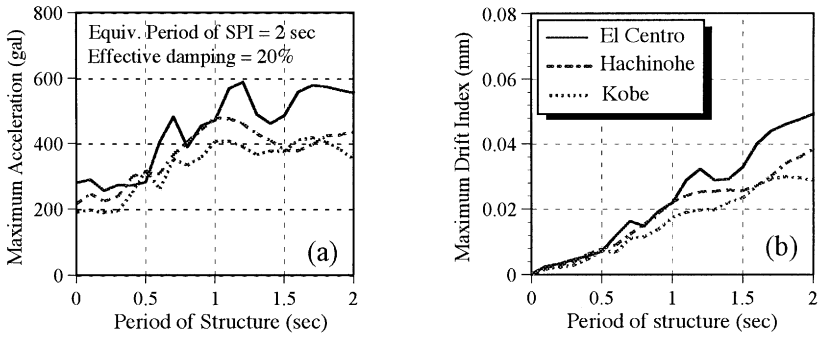

Figure 20. Spectral responses of isolated structure and its SPI isolator versus structural natural period under three excitations normalized to peak acceleration of 1000 gal

supported by the SPI system. The SPI isolator is supposed to have a fundamental period of 2 s and an effective damping ratio of 20 per cent of critical. The damping ratio of the structure is kept fixed at 0·02 of its critical damping. Since passive base isolation idea appeared to solve the problem of relatively stiff structures, the period range of 0–2·0 s is merely considered.

Figure 20 shows the peak absolute acceleration and peak lateral drift index responses of the isolated structure as a function of natural period of structure (T_s). It is observed that structural responses under El Centro excitation almost dominate the peak values for the entire range of period.

As shown in Figure 20(a), peak acceleration responses remain under 300 gal (30 per cent of input peak acceleration) for $T_s < 0{\cdot}5$ s. Further increase in the natural period of structure, increases its peak responses increasingly, up to T_s of 1·0 s. Nevertheless, the spectral acceleration responses remain under the bound of 500 gal for this desirable range of T_s between 0·0 and 1·0 s.

Figure 20(b) indicates that peak inter-storey drift indices of structure for all excitations are very similar when T_s is less than 0·5 s. This figure also shows that for $T_s \leqslant 1{\cdot}0$ s drift indices are less than 0·02 which corresponds to the serviceability limit of design criteria for strong levels of excitations. It may be interesting to notice that results of this study verified that variation of fundamental period of structure has no considerable influence on the response of the isolation system.

CONCLUSIONS

The ultimate objective of the present paper was to evaluate the dynamic responses and characteristics of the new Suspended Pendulum Isolation (SPI) device which is believed can be used as an alternative way of Laminated Rubber bearing system. To achieve this purpose, an experimental survey on a $\frac{4}{25}$-scaled model installed on a shaking-table consisting of a test structure supported on the SPI system accompanying a lead damper of various yield strength levels had been carried out.

The SPI system filtered out properly all the frequency contents of exciting earthquakes and as a result it responded in its predetermined period. Since the period of system was designed to be away from the region that most of earthquakes are strong, peak responses of the isolated structure were decreased considerably while large displacement occurred at the bearing base.

Integrating the U-shaped lead damper with the SPI system could increase the efficiency of the new device notably. Appropriate yield strength of the lead damper was achieved by means of minimizing the base shear coefficient and bearing displacement of the isolated system through the experiment. As a result, peak acceleration transmitted to the top of the isolated structure could be attenuated significantly. Meanwhile, peak base (bearing) displacement remained in the completely safe range of isolator capacity under strong

level of excitations. Furthermore, maximum drift indices of isolated test structure qualified satisfactorily the serviceability limit of design criteria.

The system had stable characteristics regardless of amplitude of oscillation. This was assessed through repeating tests under several excitations and observing a very slight difference between the first and last results even for relatively large amplitudes. The performance of the system under sinusoidal waves at resonant period gave another support for reliability of the system. Evidently, the SPI system is a reliable method to be used in actual structures, particularly in low-rise buildings.

Special attention was also paid to the determination of the dynamic response of the system analytically. The proposed model based on force–displacement characteristic validated by experiment was able to predict well not only peak values but the entire pattern of time-history responses. The results of hysteresis loop were also correlated satisfactorily with shaking-table results for each of the excitations.

ACKNOWLEDGEMENTS

This study was initiated by funding support of Dainihondoboku Co. and proceeded under sponsorships of the Japan Ministry of Education as part of international joint project titled 'Joint Study on the Mitigation of Earthquake Hazards' with grant number G08044152 (chairman: T. Shimazu). Both supports are gratefully acknowledged.

Authors are thankful to Mr. I. Narimatsu and Miss. M. Nakagawa, graduate students of Hiroshima university, whose experimental data was partially used in this paper. Also, Mr. T. Konishi, who is currently senior managing director of Dainihondoboku construction Co. is gratefully acknowledged, for his particular comments in the preliminary stage of developing the SPI device.

REFERENCES

1. J. M. Kelly, 'Aseismic base isolation: review and bibliography', *Soil Dyn. Earthquake Eng.* **5**, 202–216 (1986).
2. M. Izumi, 'Base isolation and passive seismic response control—state-of-the art report', *Proc. 9th World Conf. on Earthquake Eng.*, Vol. 8, Tokyo, Japan, 1988, pp. 385–396.
3. G. Ahmadi, 'Overview of base isolation, passive and active vibration control strategies for aseismic design of structures', *Proc. 2nd Int. Conf. on Seismology and Earthquake Engineering*, Tehran, I.R. of Iran, 1995, 1095–1125.
4. J. M. Kelly, 'Seismic isolation engineering', *Proc. 2nd Int. Conf. on Seismology and Earthquake Eng.*, Tehran, I.R. of Iran, 1995, pp. 1075–1094.
5. J. M. Kelly, 'Base isolation in Japan, *EERC Report No. 88/20*, Earthquake Engineering Research Center, University of California at Berkeley, 1988.
6. I. G. Buckle and R. L. Mayes, 'Seismic isolation: history, application, and performance—a world view', *Earthquake Spectra* **6**, 161–201 (1990).
7. R. I. Skinner, W. H. Robinson and G. H. McVerry, *An Introduction to Seismic Isolation*, Wiley, New York, 1993.
8. F.-G. Fan, G. Ahmadi, N. Mostaghel and I. G. Tadjbakhsh, 'Performance analysis of aseismic base isolation systems for a multi-storey building', *Soil Dyn. Earthquake Eng.* **10**, 152–171 (1991).
9. A. V. Zayas, S. S. Low and S. A. Mahin, 'A simple pendulum technique for achieving seismic isolation', *Earthquake Spectra* **6**, 317–333 (1990).
10. A. Mokha, M. C. Constantinou, A. M. Reinhorn and A. Zayas, 'Experimental study of friction-pendulum isolation system', *Struct. Engng. ASCE* **117**, 1201–1217 (1991).
11. T. Shimazu, T. Konishi, H. Araki and I. Narimatsu, 'Development of a new device of base isolation system by hanging up buildings: part 1 and 2', Summaries of Technical Papers of AIJ Annual Meeting, Vol. B-2, 1995, pp. 609–612 (in Japanese).
12. A. Bakhshi, T. Shimazu, H. Araki and I. Narimatsu, 'Dynamic characteristics of a new pendulum isolation system', Technical Report of Chugoku-Kyushu Joint Branch of AIJ, Vol. 10, 1996, pp. 221–224.
13. A. Bakhshi, H. Araki and T. Shimazu, 'Application of base isolation system in bridges; from design and analysis perspective views', *Proc. 2nd Int. Conf. on Bridges*, Tehran, I.R. of Iran, September 1996, pp. 101–110.
14. I. Narimatsu, T. Shimazu, H. Araki and T. Konishi, 'Development of a new device of base isolation system by hanging up buildings: Part 3', Technical Report of Chugoku Branch of AIJ, Vol. 19, 1995, pp. 69–72 (in Japanese).
15. M. Nakagawa, T. Shimazu, T. Konishi, H. Araki and A. Bakhshi, 'Development of a new device of base isolation system by hanging up buildings: part 3 and 4', Summaries of Technical Papers of AIJ Annual Meeting, Vol. B-2, 1996, pp. 753–756 (in Japanese).
16. K. Dekker and J.G. Verwer, *Stability of Runge–Kutta Methods for Stiff Nonlinear Differential Equations*, North-Holland, Amsterdam, 1984.
17. Architectural Institute of Japan (AIJ), *Recommendation for the Design of Base Isolated Buildings*, 1993 (in Japanese).
18. M. Paz, *International Handbook of Earthquake Engineering: Codes, Programs, and Examples*, Chapman and Hall, New York, 1994.
19. F. Naeim, *The Seismic Design Hand Book*, Van Nostrand Reinhold, New York, 1989.

